EURASIP Journal on Applied Signal Processing 2005:4, 532–540

Low-Complexity Blind Symbol Timing Offset Estimation in OFDM Systems

Tiejun Lv
School of Information Engineering, Beijing University of Posts and Telecommunications, Beijing 100876, China
Email: lvtiejun@tsinghua.org.cn

Jie Chen
Division of Engineering, Brown University, Providence, RI 02912, USA
Email: jie_chen@brown.edu

Hua Li
Division of Engineering, Brown University, Providence, RI 02912, USA
Email: hua_li_1@brown.edu

Received 19 February 2004; Revised 4 October 2004; Recommended for Publication by Marc Moonen

A low-complexity blind timing algorithm is proposed to estimate timing offset in OFDM systems when multiple symbols are received (the timing offset estimation is independent of the frequency offset one). Though the maximum-likelihood estimation (MLE) using two or three symbols is good in offset estimation, its performance can be significantly improved by including more symbols in our previous work. However, timing offset estimation requires *exhaustive search* and a priori knowledge of the probability distribution of the received data. The method we propose utilizes the second-order statistics embedded in a cyclic prefix. An *information vector* (IVR) with the same length as the cyclic prefix is formed based on an *autocorrelation matrix* (AM). The modulus of elements in the IVR is first quantized based on a threshold that is defined by the variance of OFDM symbols. The timing offset is then estimated based on the binary sequence of the IVR. Because the exhaustive search used in the MLE can be avoided, computational complexity is significantly reduced. In practice, the proposed scheme can be used as a coarse synchronization estimation that can rapidly provide a rough and contractible estimation range, which serves as the basis for a fine estimation like the MLE. The proposed estimator will be proved theoretically to be asymptotically unbiased and mean-squared consistent. Simulations and comparisons will be provided in the paper to illustrate the advantages of our design.

Keywords and phrases: symbol timing offset estimation, maximum-likelihood estimation, frequency offset estimation, blind estimation in OFDM communications.

1. INTRODUCTION

With the advances of wireless technologies, wireless networking has become ubiquitous due to the growing demand for pervasive mobile applications. It is projected that one-fifth of the world's population will access the Internet by mobile phone by the end of 2004. The convergence of computing, communication, and media will allow the users to communicate with each other and access any content *at any time, anywhere*. Future wireless networks will support services such as high-speed access, telecommuting, interactive media, video conferencing, real-time Internet gaming, e-business ecosystems, smart homes, automated highways, and disaster relief. Yet we still have to overcome many technical challenges in order to make this vision of a wireless future into reality. For instance, the performance of 3G wireless systems is not sufficient to meet the needs of future high-performance multimedia applications. There is thus a demand to extend the capabilities of current 3G wireless systems to the so-called "IP-based 4G systems." Among the 4G systems, the orthogonal frequency division multiplexing (OFDM) technique is probably the most promising technique for providing high-throughput broadband services. The OFDM is a multicarrier scheme of digital modulation and has been applied to terrestrial digital audio broadcasting (DAB) and digital video broadcasting (DVB) [1, 2]. The OFDM increases symbol duration by dividing an entire channel into many narrowband subchannels that are orthogonal to each other. The high-rate serial data stream is divided into many low-rate parallel streams. It can provide high spectral efficiency, and can also produce much greater immunity to impulse noise and multipath fading. Its performance can be significantly improved

using only a simple equalization technique [3]. Assuming that the length of the guard interval is larger than the delay spread of a channel, we can achieve communications without intersymbol interference (ISI) by inserting a cyclic prefix (also known as guard interval) into OFDM symbols [4]. Compared to the single-carrier system, the OFDM system is more sensitive to symbol timing error and frequency offset. This sensitiveness can cause significant system performance deterioration. To alleviate this problem, symbol timing and frequency offset must be accurately estimated and compensated for at a receiver before demodulation [5].

There are two major categories of timing and frequency correction techniques in OFDM systems, *data-aided* and *non-data-aided* estimation (also known as *blind estimation*). Data-aided techniques use a known bit pattern or a pilot signal to estimate timing or frequency offset [6, 7]. However, in the data-aided design, some specialized synchronization symbols must be transmitted through a control channel, reducing achievable data rate. Non-data-aided blind estimation techniques offer another promising design alternative. These techniques estimate the synchronization parameters based on received information and utilize the side information consisting of incoming signal statistics. A maximum-likelihood estimation (MLE) technique was presented in [8] and later modified in [9]. Two or three OFDM frames (symbols) are used in [9] for estimation, and this technique's performance can be further improved by averaging over more symbols [10]. It has been proved that extending the observation interval can lead to improved estimation accuracy [11]. The previously mentioned estimations, however, need to perform an exhaustive search that requires high computational complexity.

So far, the majority of symbol timing offset estimation schemes are based on the assumption that an additive white Gaussian noise (AWGN) channel is present. The main reason for this is that signals that passed through a multipath dispersive channel have a much more complicated correlation structure than those passed through an AWGN channel. Although the author in [12] claims that signals in the model are transmitted over a fast Rayleigh-fading channel, the estimation model is actually derived from a single-path Rayleigh-fading channel. It *does not* actually differ from the AWGN channel model and *is not* suitable for estimation over a multipath channel. In this paper, we also assume that the channel is AWGN for simplicity. We have proposed a complicated estimation design for a fast time-varying *multipath* channel in [13].

Timing offset estimation is usually performed before carrier frequency recovery is completed. Popular carrier frequency offset estimation schemes require perfect timing synchronization [14, 15, 16]. In this paper, we propose a new but simple timing offset estimator. A novel non-data-aided structure based on cyclic prefix has been introduced to estimate timing offset, and the proposed algorithm is independent of the frequency offset in OFDM systems. In our design, an information vector (IVR) is defined as a vector with the same length as a guard interval, which consists of elements in the off-diagonal submatrix of a sample autocorrelation matrix (AM). The IVR can provide sufficient information for offset-parameters estimation. Elements within the IVRs are first quantized into "0" or "1" based on a threshold defined by the variance of OFDM symbols. The timing offset can then be estimated based on the trend (rising edge or falling edge) of a quantized IVR, and based on the number of "0's" or "1's" within the IVR. Our proposed scheme does not require any probability assumptions about the received data and its signal-to-noise ratio (SNR). The frequency offset can be estimated by the phase angle of elements within an IVR. Because the exhaustive search is avoided, the computational complexity of the proposed estimator is significantly reduced. We will provide the numerical analysis later in this paper to demonstrate the performance of our design. The proposed method can actually be combined with a MLE mechanism for offset estimation, the proposed method for coarse estimation and the method combined with MLE for fine estimation. The scalable design provides a tradeoff between estimation complexity and accuracy. We will prove theoretically that the proposed estimator is asymptotically unbiased and mean-squared consistent.

The rest of this paper is organized as follows. In Section 2, we briefly survey the scientific background to our design, including the OFDM system, and also describe our design assumptions. Then, we introduce the proposed symbol timing and frequency offset estimators in Section 3. In Section 4, the numerical analysis of the proposed estimators will be discussed. Simulation results over an AWGN channel or a time-varying multipath channel will be presented in Section 5. Finally, we conclude our paper in Section 6.

2. SCIENTIFIC BACKGROUND

To simplify our analysis, we have chosen to investigate an N-subcarrier OFDM system over an AWGN channel. For comparison, we will evaluate our estimator's performance over both the AWGN channel and a time-varying multipath channel. A basic block diagram of an OFDM system is given in Figure 1. On the transmitter side, N complex data symbols are modulated onto N subcarriers using the inverse fast fourier transform (IFFT). The last N_g samples of the IFFT outputs are copied and inserted at the beginning of each OFDM symbol (e.g., one frame or one block) to form a guard interval. A baseband-modulated signal $s(n)$ is available after the parallel-to-serial conversion, and can be expressed as

$$s(n) = \sum_{l=-\infty}^{+\infty} \sum_{k=0}^{N-1} S_k(l) e^{j2\pi k(n-N_g-lM)/N} \operatorname{rect}(n - lM), \quad (1)$$

where $S_k(l)$ is a data symbol modulated by the kth subcarrier during the lth OFDM symbol duration. $M = N + N_g$, and $S_k(l)$ is a zero-mean random variable with correlation $E\{S_k(l)S_{k'}^*(l')\} = \sigma_s^2\delta(k-k')\delta(l-l')$. In the previous equations, $*$ is a conjugate operator. $\operatorname{rect}(\cdot)$ is a rectangular function written as follows:

$$\operatorname{rect}(n) = \begin{cases} 1, & 0 \le n \le M-1, \\ 0, & \text{elsewhere.} \end{cases} \quad (2)$$

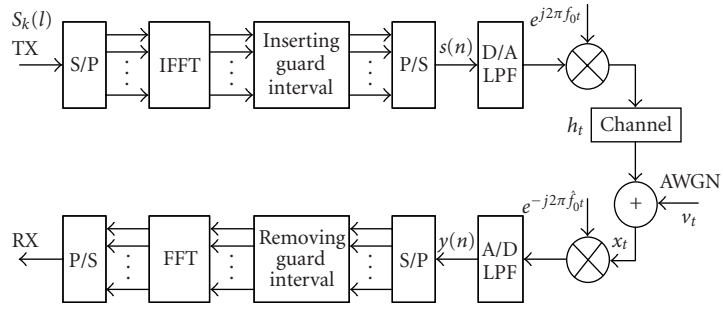

Figure 1: Block diagram of an OFDM system.

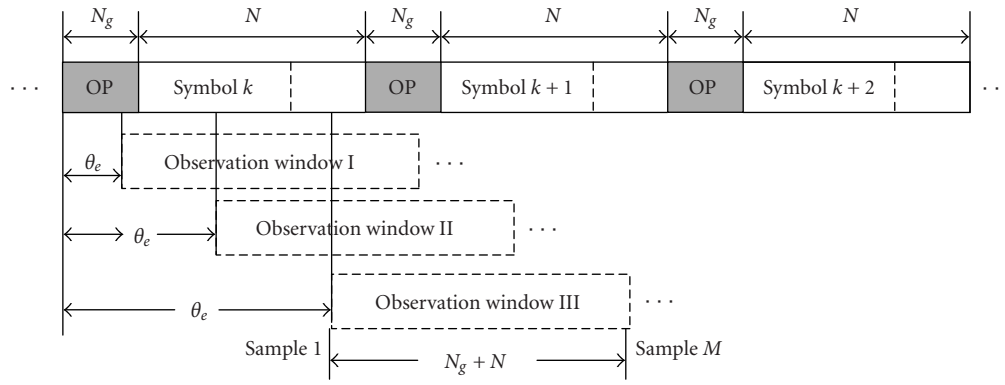

Figure 2: Different positions of observation windows in an OFDM frame.

On the receiver side, the timing uncertainty in an OFDM signal can be modeled as a time shift $\theta_e \in \mathbb{Z}$, where $\mathbb{Z}$ is an integer set. The unknown carrier frequency offset, which is caused by the Doppler effect and inherent instabilities in the transmitter and/or receiver carrier frequency oscillators, is expressed as a frequency shift, ε. The received signal can be written as

$$y(n) = s(n+\theta_e)e^{j2\pi\varepsilon n/N} + v(n), \tag{3}$$

where $v(n)$ is an AWGN noise with zero-mean and variance σ_v^2. Next, we will develop a novel low-complexity approach to estimate both the timing and frequency offsets in OFDM systems.

3. ESTIMATION OF TIMING OFFSET

Assume that $\mathbf{z}(n) = [z(n), z(n+1), \ldots, z(n+M-1)]^T$ is an $M \times 1$ ($M = N_g + N$) observation column vector received at time n, and $z(k) = y(k-M+1)$. The start of a received OFDM symbol can probably occur anywhere within a symbol duration because sampling instants are randomly generated (refer to Figure 2), namely, $\theta_e \in \{0, 1, 2, \ldots, M-1\}$. The timing error θ_e can be divided into three different cases over an OFDM symbol, as shown in Figure 2. The structure of an AM highly depends on the timing error.

Case 1 ($0 \le \theta_e < N_g$). In this case, the AM can be expressed as

$$\mathbf{R} = \begin{bmatrix} \mathbf{A}_1 & \mathbf{0} & \mathbf{B} \\ \mathbf{0} & \mathbf{A}_2 & \mathbf{0} \\ \mathbf{B}^H & \mathbf{0} & \mathbf{A}_1 \end{bmatrix}, \tag{4}$$

where $\mathbf{A}_1 = \text{diag}[\sigma_s^2 + \sigma_v^2, \ldots, \sigma_s^2 + \sigma_v^2]$ is an $N_g \times N_g$ matrix, $\mathbf{A}_2 = \text{diag}[\sigma_s^2 + \sigma_v^2, \ldots, \sigma_s^2 + \sigma_v^2]$ is of dimension $(N - N_g) \times (N - N_g)$, and

$$\mathbf{B} = \text{diag}\,[\underbrace{\sigma_s^2 e^{-j2\pi\varepsilon}, \ldots, \sigma_s^2 e^{-j2\pi\varepsilon}}_{N_g-\theta_e}, \underbrace{0, \ldots, 0}_{\theta_e}], \tag{5}$$

$\mathbf{B}$ is an $N_g \times N_g$ matrix. σ_s^2 is the variance of $s(n)$, and $(\cdot)^H$ denotes a conjugate transpose operation. Obviously, only the main diagonal entries of the matrix $\mathbf{B}$, the so-called "IVR" in our design, contain information on timing error and frequency offset. The rest of the AM is independent of these offsets.

Case 2 ($N_g \le \theta_e < N$). In this case, the AM can be expressed as follows:

$$\mathbf{R} = \text{diag}\,[\sigma_s^2 + \sigma_v^2, \ldots, \sigma_s^2 + \sigma_v^2], \tag{6}$$

where matrix $\mathbf{R}$ has the dimension of $(N + N_g) \times (N + N_g)$.

It does not contain any information about the timing offset θ_e and frequency offset ε. However, the observation window can be shifted by a multiple of N_g samples to the right or the left, which eventually leads to the same scenario as in Case 1 or Case 3.

Case 3 ($N \le \theta_e < N + N_g$). In this case, the AM can be expressed in the following form:

$$\mathbf{R} = \begin{bmatrix} \mathbf{A}_1 & \mathbf{0} & \mathbf{C} \\ \mathbf{0} & \mathbf{A}_2 & \mathbf{0} \\ \mathbf{C}^H & \mathbf{0} & \mathbf{A}_1 \end{bmatrix}, \tag{7}$$

where

$$\mathbf{C} = \operatorname{diag}\big[\underbrace{0,\ldots,0}_{M-\theta_e-1}, \underbrace{\sigma_s^2 e^{-j2\pi\varepsilon},\ldots,\sigma_s^2 e^{-j2\pi\varepsilon}}_{\theta_e-N+1}\big], \tag{8}$$

$\mathbf{C}$ is an $(N_g \times N_g)$-dimensional matrix. Similarly to Case 1, only the IVR consisted of the main diagonal entries of matrix $\mathbf{C}$ contains synchronization parameters. It provides sufficient information to calculate the timing and frequency offsets. Notice that the order of zero entries in matrix $\mathbf{C}$ is different from those in matrix $\mathbf{B}$ in (5), which helps timing offset estimator to distinguish Case 1 from Case 3.

The algorithm to estimate timing error can be summarized in Algorithm 1.

Where the threshold Λ exists, the quantized vector $\mathbf{r}$ is defined as $\sigma_s^2/2$. This is because the expected distance between the two kinds of the elements' absolute values in the IVR $\mathbf{r}$ is σ_s^2. The boundary classified the two kinds of the elements can thus be set as half of the distance, that is, $\sigma_s^2/2$.

To better illustrate the algorithm, we include a flow chart in Figure 3. Our estimation algorithm does not require any exhaustive search. In Cases 1 and 3, the estimator can directly compute a closed-form solution of the timing offset. In Case 2, at most $N/N_g - 1$ searches are required to obtain the estimation.

Frequency offset is estimated after timing offset. However, the performance evaluation of frequency offset estimator is beyond the scope of this paper (please refer to [8, 9, 10, 11] for the detailed discussion). In this paper, we will focus on frequency offset estimation.

Assuming that $\widetilde{\mathbf{R}}$ is an AM calculated according to received data, and its timing error can be perfectly corrected, $\widetilde{\mathbf{R}}$ can be expressed as

$$\widetilde{\mathbf{R}} = \begin{bmatrix} \widetilde{\mathbf{A}}_1 & \mathbf{0} & \widetilde{\mathbf{B}} \\ \mathbf{0} & \widetilde{\mathbf{A}}_2 & \mathbf{0} \\ \widetilde{\mathbf{B}}^H & \mathbf{0} & \widetilde{\mathbf{A}}_1 \end{bmatrix}, \tag{9}$$

where $\widetilde{\mathbf{A}}_1 = \operatorname{diag}[\sigma_s^2 + \sigma_v^2,\ldots,\sigma_s^2 + \sigma_v^2]$ is an $N_g \times N_g$ matrix and $\widetilde{\mathbf{A}}_2 = \operatorname{diag}[\sigma_s^2 + \sigma_v^2,\ldots,\sigma_s^2 + \sigma_v^2]$ has the dimension of $(N - N_g) \times (N - N_g)$.

$$\widetilde{\mathbf{B}} = \operatorname{diag}\big[\underbrace{\sigma_s^2 e^{-j2\pi\varepsilon},\ldots,\sigma_s^2 e^{-j2\pi\varepsilon}}_{N_g}\big] \tag{10}$$

Input—an observation column vector $\mathbf{z}(n)$.
Output—symbol timing offset $\hat{\theta}_e$.
Begin
(1) Calculate the IVR $\mathbf{r}$ that is made up of the main diagonal entries of the top right $N_g \times N_g$ submatrix of the AM $\mathbf{R}$.
(2) Calculate the quantized vector $\mathbf{r}'$. Vector $\mathbf{r}$ is quantized to "0" if its absolute value is below the threshold $\Lambda = \sigma_s^2/2$; otherwise, it is quantized to "1." In this way, vector $\mathbf{r}$ can be rewritten as vector $\mathbf{r}'$, which is given 0 or 1.
(3) Decide whether or not all the elements of vector $\mathbf{r}'$ are zero. If yes, skip to step (5); otherwise, proceed to the next step (step (4)).
(4) Determine the trend of 0 and 1 entries in the quantized IVR $\mathbf{r}'$. If it is a falling trend, with a pattern of leading 1's followed by 0's, as in $\mathbf{r}' = [\underbrace{1,1,\ldots,1}_{N_g-\theta_e}, \underbrace{0,0,\ldots,0}_{\theta_e}]$, we can determine that it is Case 1. We can get $\hat{\theta}_e = N_0$, where N_0 is the number of "0" elements in $\mathbf{r}'$; otherwise, if it follows a rising trend, with a pattern of leading 0's followed by 1's, as in $\mathbf{r}' = [\underbrace{0,0,\ldots,0}_{M-\theta_e-1}, \underbrace{1,1,\ldots,1}_{\theta_e-N+1}]$, it belongs to Case 3 and $\hat{\theta}_e = M - N_0 - 1$. We can then jump to step (6).
(5) After shifting the observation window by N_g samples to the right, we recalculate the quantized IVR $\mathbf{r}'$, and repeat this procedure until Case 3 appears. Assuming the number of times shifted is n_m, we can calculate the timing offset $\hat{\theta}_e = M - N_0 - n_m N_g$.
(6) Correct the timing error θ_e. End of the algorithm.

Algorithm 1: Low-complexity blind symbol timing offset estimation algorithm.

is a matrix with dimension of $N_g \times N_g$. We define matrix $\mathbf{D} = \angle(\widetilde{\mathbf{B}})$, where $\angle(\cdot)$ is a phase angle function for every entry in $\widetilde{\mathbf{B}}$. The frequency offset estimator $\hat{\varepsilon}$ can then be expressed as

$$\hat{\varepsilon} = \frac{-1}{2\pi N_g}\big(\operatorname{tr}(\mathbf{D})\big), \tag{11}$$

where $\operatorname{tr}(\mathbf{D})$ denotes the trace of matrix $\mathbf{D}$. A residual timing offset $\Delta\theta_e$ always exists and causes the frequency offset estimation's performance to deteriorate. In general, we can assume $\Delta\theta_e \in \{1, 2, \ldots, N_g - 1\}$. Here $\widetilde{\mathbf{B}}$ becomes

$$\widetilde{\mathbf{B}} = \operatorname{diag}\big[\underbrace{\sigma_s^2 e^{-j2\pi\varepsilon},\ldots,\sigma_s^2 e^{-j2\pi\varepsilon}}_{N_g-\Delta\theta_e}, \underbrace{0,\ldots,0}_{\Delta\theta_e}\big]. \tag{12}$$

In order to reduce the frequency offset estimation error, we have

$$\hat{\varepsilon} = \frac{-1}{2\pi}\angle\big(\operatorname{tr}(\widetilde{\mathbf{B}})\big) \tag{13}$$

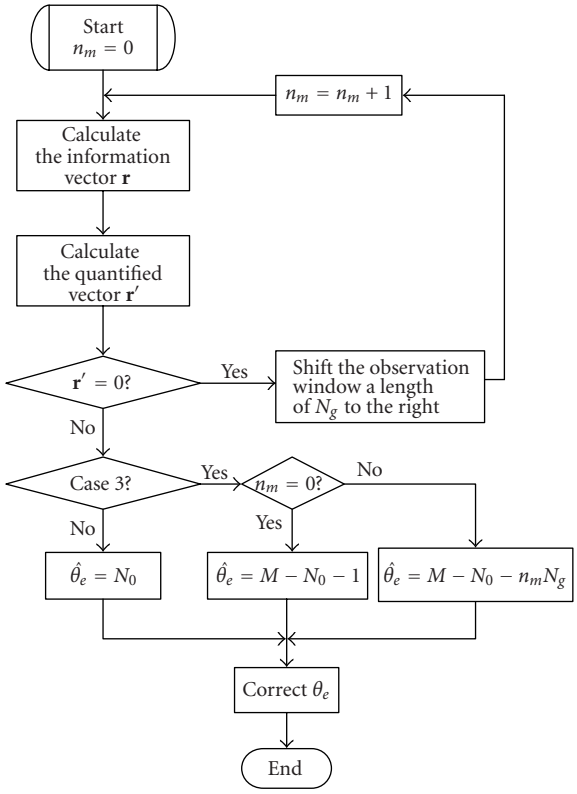

Figure 3: Flow chart of the proposed algorithm.

or

$$\hat{\varepsilon} = \frac{-1}{2\pi}\angle(\widetilde{\mathbf{B}}_{1,1}), \tag{14}$$

where $\widetilde{\mathbf{B}}_{1,1}$ denotes the entry in the first row and the first column of the matrix $\widetilde{\mathbf{B}}$.

4. PERFORMANCE AND COMPUTATIONAL COMPLEXITY ANALYSIS

The AM $\mathbf{R}$ can be estimated as follows:

$$\hat{\mathbf{R}} = \frac{1}{L_f}\sum_{l=0}^{L_f-1}\mathbf{z}(lM)\mathbf{z}^H(lM), \tag{15}$$

where L_f is the number of observation frames. It is asymptotically unbiased and mean-squared consistent [14]. From the proposed algorithm in Section 3, we can write the timing offset estimator $\hat{\theta}_e$ in Case 1 as follows:

$$\hat{\theta}_e = \sum_{k=1}^{N_g} U\left(\left|\bar{r}(k)\right| \le \frac{\sigma_s^2}{2}\right), \tag{16}$$

where $\bar{\mathbf{r}} = [\bar{r}(1), \bar{r}(2), \ldots, \bar{r}(N_g)]$ and $\bar{\mathbf{r}}$ is the estimation of an IVR $\mathbf{r}$. The function $U(\cdot)$ is used for quantization, which can be written as

$$U\left(\left|\bar{r}(k)\right| \le \frac{\sigma_s^2}{2}\right) = \begin{cases} 1, & \left|\bar{r}(k)\right| \le \dfrac{\sigma_s^2}{2}, \\ 0, & \text{else.} \end{cases} \tag{17}$$

According to (16), we can easily verify that this estimator is asymptotically unbiased in Case 1 as follows:

$$\begin{aligned} \lim_{L_f\to+\infty} E\{\hat{\theta}_e\} &= \lim_{L_f\to+\infty}\sum_{k=1}^{N_g} E\left\{U\left(\left|\bar{r}(k)\right| \le \frac{\sigma_s^2}{2}\right)\right\} \\ &= \lim_{L_f\to+\infty}\sum_{k=1}^{N_g}\Pr\left(\left|\bar{r}(k)\right| \le \frac{\sigma_s^2}{2}\right) = \theta_e. \end{aligned} \tag{18}$$

The variance of the timing offset estimator $\hat{\theta}_e$ in Case 1 can be written as

$$\begin{aligned} \lim_{L_f\to+\infty}\mathrm{Var}\{\hat{\theta}_e\} &= \lim_{L_f\to+\infty}\left\{E\{\hat{\theta}_e^2\} - E^2\{\hat{\theta}_e\}\right\} \\ &= \lim_{L_f\to+\infty} E\{\hat{\theta}_e^2\} - \theta_e^2. \end{aligned} \tag{19}$$

The first term on the right-hand side of (19) can be rewritten as

$$\begin{aligned} &\lim_{L_f\to+\infty} E\{\hat{\theta}_e^2\} \\ &= \lim_{L_f\to+\infty}\sum_{k_1=1}^{N_g}\sum_{k_2=1}^{N_g} E\left\{U\left(\left|\bar{r}(k_1)\right| \le \frac{\sigma_s^2}{2}\right)\cdot U\left(\left|\bar{r}(k_2)\right| \le \frac{\sigma_s^2}{2}\right)\right\} \\ &= \lim_{L_f\to+\infty}\sum_{k_1=1}^{N_g}\sum_{k_2=1}^{N_g}\Pr\left\{\left(\left|\bar{r}(k_1)\right| \le \frac{\sigma_s^2}{2}\right)\cap\left(\left|\bar{r}(k_2)\right| \le \frac{\sigma_s^2}{2}\right)\right\} \\ &= \lim_{L_f\to+\infty}\left\{\sum_{k_1=1}^{N_g}\Pr\left(\left|\bar{r}(k_1)\right| \le \frac{\sigma_s^2}{2}\right)\cdot\sum_{k_2=1}^{N_g}\Pr\left(\left|\bar{r}(k_2)\right| \le \frac{\sigma_s^2}{2}\right)\right\} \\ &= \theta_e^2. \end{aligned} \tag{20}$$

By substituting (20) into (19), we have

$$\lim_{L_f\to+\infty}\mathrm{Var}\{\hat{\theta}_e\} = 0. \tag{21}$$

Therefore, the timing offset estimator $\hat{\theta}_e$ is mean-squared consistent with increasing L_f in Case 1. Similarly, we can prove that the timing-offset estimator $\hat{\theta}_e$ is asymptotically unbiased and mean-squared consistent in Cases 2 and 3. Since the frequency offset estimator $\hat{\varepsilon}$ is a deterministic function of $\bar{r}(k)$, which is asymptotically unbiased and consistent, we conclude that $\hat{\varepsilon}$ is also an asymptotically unbiased and a consistent estimator of ε.

To demonstrate the low-complexity of our proposed design, we would like to compare the computational complexity of the proposed scheme with an MLE design in [11].

To simplify the comparison, we can rewrite the timing offset estimator in [11] as

$$\hat{\theta}_e = \arg\max_{\theta_e} \left(2\left|T_1(\theta_e)\right| - \rho T_2(\theta_e)\right), \tag{22}$$

where $\rho = \sigma_s^2/(\sigma_s^2 + \sigma_v^2)$,

$$T_1(\theta_e) = \begin{cases} \displaystyle\sum_{k=\theta_e'}^{\theta_e+N_g-1} \sum_{l=0}^{L_f-2} z(k+lM)\cdot z^*(k+lM+N), \\ \qquad 1 \le \theta_e \le N, \\ \displaystyle\sum_{k=0}^{\theta_e-N-1} z(k)\cdot z^*(k+N) \\ \quad + \displaystyle\sum_{k=\theta_e}^{\theta_e+N_g-1} \sum_{l=0}^{L_f-2} z(k+lM)\cdot z^*(k+lM+N), \\ \qquad N+1 \le \theta_e \le M, \end{cases}$$

$$T_2(\theta_e) = \begin{cases} \displaystyle\sum_{k=\theta_e'}^{\theta_e+N_g-1} \sum_{l=0}^{L_f-2} \left(\left|z(k+lM)\right|^2 + \left|z(k+lM+N)\right|^2\right), \\ \qquad 1 \le \theta_e \le N, \\ \displaystyle\sum_{k=0}^{\theta_e-N-1} \left(\left|z(k)\right|^2 + \left|z(k+N)\right|^2\right) \\ \quad + \displaystyle\sum_{k=\theta_e}^{\theta_e+N_g-1} \sum_{l=0}^{L_f-2} \left(\left|z(k+lM)\right|^2 + \left|z(k+lM+N)\right|^2\right), \\ \qquad N+1 \le \theta_e \le M. \end{cases} \tag{23}$$

Here we assume that the computational complexity for calculating an IVR is N_c. From Section 3, we know that it requires at most $N/N_g - 1$ searches to estimate the timing offset in the $N_g \le \theta_e < N$ case. The maximum computational complexity is $N_c(N/N_g - 1)$. From (22) and (23), we can see that the computational complexity to estimate a given θ_e in [11] is approximately $2N_c$. This method requires an exhaustive search of $N + N_g$ over each symbol interval. As a result, the total computational complexity of this method is $2N_c(N + N_g)$. We can define a complexity coefficient η as

$$\begin{aligned} \eta &= \frac{\text{the computation complexity of our algorithm}}{\text{the computation complexity in [11]}} \\ &= \frac{N - N_g}{2N_g(N + N_g)}, \end{aligned} \tag{24}$$

when $N \gg N_g$, $\eta \approx 1/(2N_g)$. The complexity of the proposed algorithm is thus at least $2N_g$ times lower than that in [11], proving that ours is a low-complexity design.

5. SIMULATION RESULTS AND COMPARISONS

In this section, we present simulation results to demonstrate the performance of the proposed timing and frequency offset estimation in OFDM systems. The OFDM model used in the simulation contains a 64-point FFT, a guard interval of 16 samples (1/4 of the useful data interval), and a 16-QAM modulation scheme. SNR is defined as SNR $= 10\log\sigma_s^2/\sigma_v^2$.

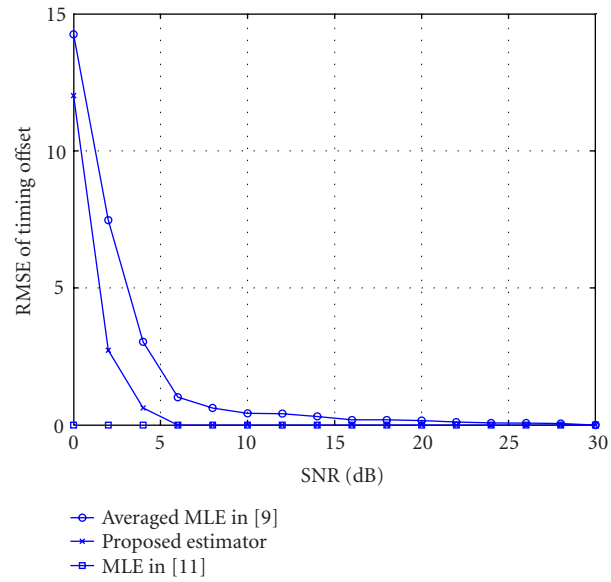

Figure 4: Comparing the performance of the timing offset estimation among the averaged MLE in [9], the proposed estimator, and the optimal MLE in [11].

To compare the performance of our proposed estimator with that of the ML estimator (MLE), we assume that $\varepsilon = 0.128$ and $\theta_e = 19$, and compute the root mean square error (RMSE) of the timing offset over SNR $= 0 \sim 30$ dB in an AWGN channel. Each simulation consists of 54 observation frames. All results have been obtained by averaging over 200 independent Monte Carlo trials. The ML methods include the MLEs in [9, 10], which average estimation results over multiple received frames; and an MLE in [11]. The MLE in [11] theoretically can achieve optimal performance given the previous assumptions. Its timing offset estimation performance is better than both the averaged MLE in [10] and our proposed estimator, as shown in Figure 4, especially when SNR < 4 dB. The performance of our timing offset estimator lies somewhere between the two MLEs, when SNR < 4 dB. Although its performance is not as good as the optimal MLE using multiple received frames in [11], its computational complexity is only 3.125% ($\eta = 0.03125$) of the estimator in [11], based on the calculation in (24). Our proposed algorithm retains acceptable estimation performance and thus can provide a coarse initial search under SNR < 4 dB condition. When SNR ≥ 4 dB, the performance of our estimator approaches that of the optimal MLE. Our scheme becomes more attractive than the MLE in [11] due to its low complexity. Figure 5 shows the frequency offset estimation performance of three different estimators and the Cramér-Rao bound (CRB) of the MLE.

An OFDM system is intended to be used in a multipath environment. We also have to consider the performance of our estimators in a time-varying multipath channel.

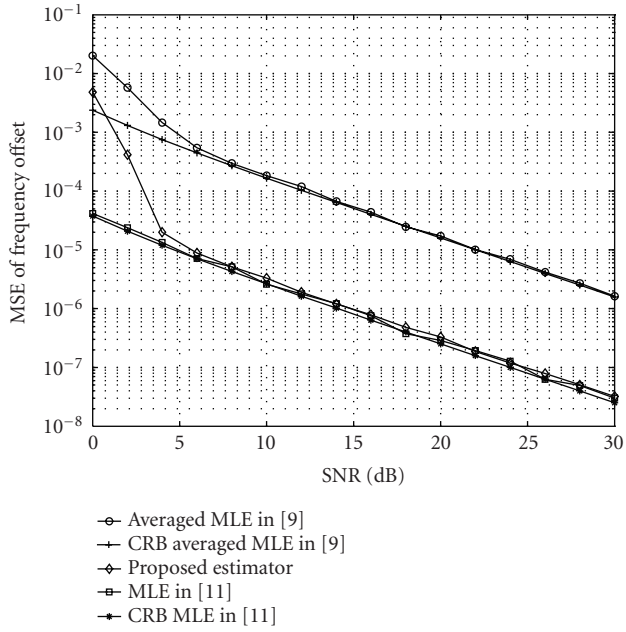

Figure 5: Comparing the performance of the frequency offset estimation among the averaged MLE in [9], the proposed estimator, and the optimal MLE in [11].

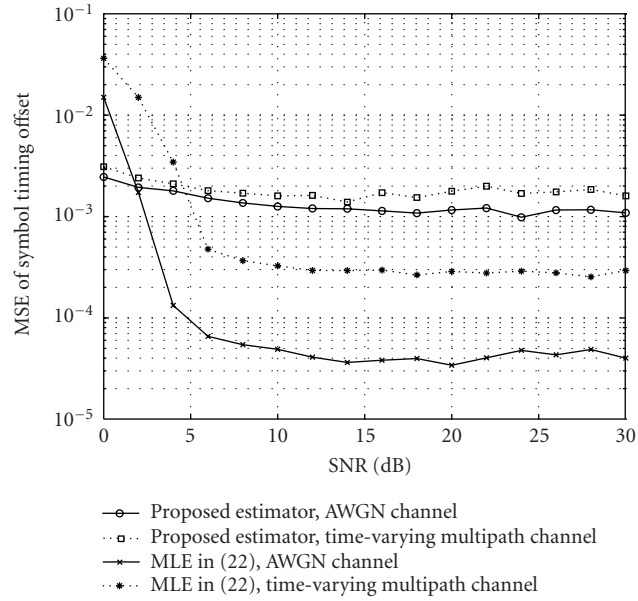

Figure 6: MSE of $\hat{\theta}_e/M$ versus θ_e/M as a function of SNR for both our estimator and the MLE with an AWGN channel and a time-varying multipath channel, respectively.

It is assumed that a delayed power spectrum follows an exponential distribution, the Doppler spectrum follows the classical model in [17], and the maximum delay spread is 10 samples. We also assume that each realization consists of 3 observation frames. All results have been obtained by averaging over 500 independent Monte Carlo trials. Figure 6 shows the mean square error (MSE) of $\hat{\theta}_e/M$ versus θ_e/M as a function of SNR for both our design and the MLE in (22) with an AWGN channel and a time-varying multipath channel, respectively. It is obvious that performance degrades for both our estimators with the time-varying multipath channel compared to performance with the AWGN channel. Figure 6 also shows that the performance of the proposed timing offset estimator is better than that of the MLE under low SNR conditions. This implies that we can combine the proposed estimator with the MLE in (22) to achieve optimal offset estimation. Specifically, the proposed estimator can serve as an initial coarse synchronization to narrow down the estimation range. The MLE fine synchronization in (22) then needs only to search over a very narrow range and obtains an accurate estimation result. This combined scheme has the merits of both designs in term of high estimation accuracy and low computational complexity.

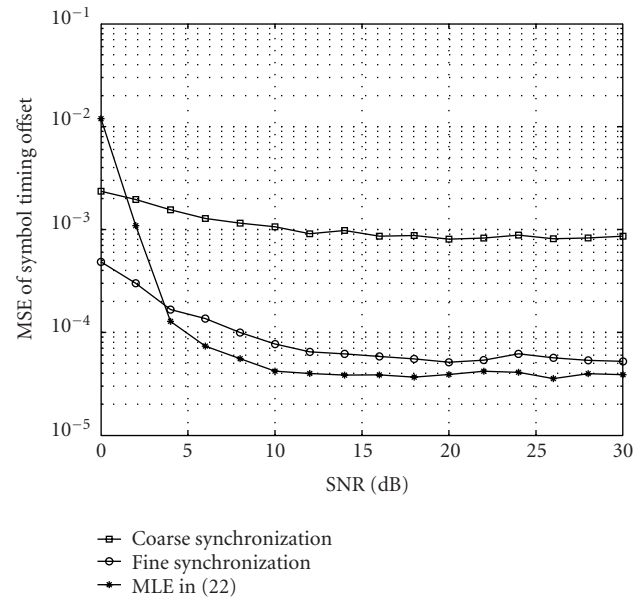

Figure 7: MSE of $\hat{\theta}_e/M$ versus θ_e/M as a function of SNR for coarse synchronization and fine synchronization with an AWGN channel, respectively.

Figure 7 shows the MSE of $\hat{\theta}_e/M$ versus θ_e/M as a function of SNR for coarse synchronization and for fine synchronization as they have been previously defined for an AWGN channel, respectively. Coarse synchronization is the one we proposed in this paper, whereas fine synchronization is the MLE algorithm, as shown in (22). In each simulation, 3 observation frames are used. Let $\hat{\theta}'_e$ denote the timing offset given by coarse synchronization. The search range of the timing offset for fine synchronization is then within $[\hat{\theta}'_e - b, \hat{\theta}'_e + b]$, where $b = 5$ is a searching radius and is far smaller than a symbol interval. From Figure 7, we observe that the proposed scheme outperforms other estimators under SNR < 4 dB conditions and gets close to the performance

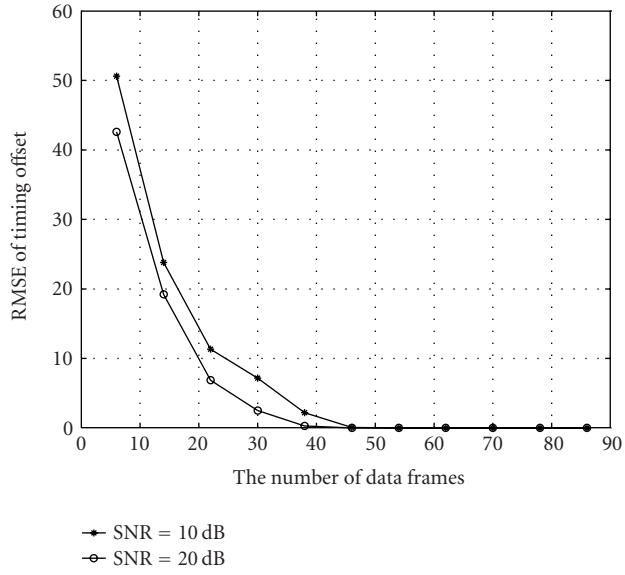

Figure 8: RMSE of our symbol timing offset estimator versus the number of frames used under different SNRs.

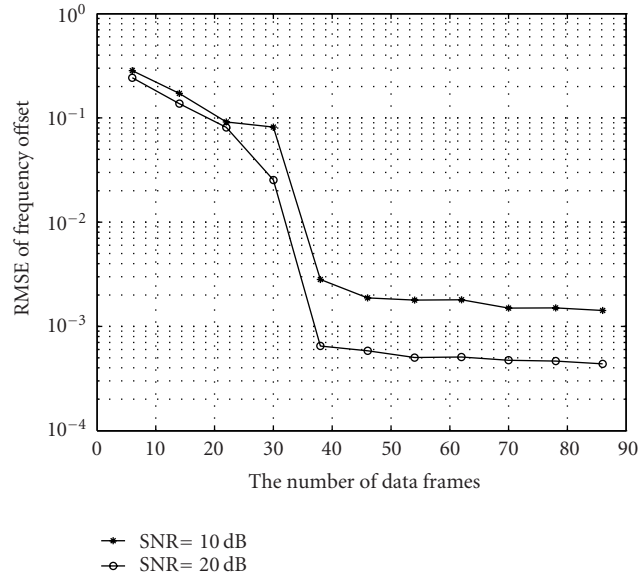

Figure 9: RMSE of the proposed frequency offset estimator versus number of frames used under different SNRs.

of the MLE in (22) under SNR $\geq$ 4 dB conditions, but its complexity is only 15.6% of that of the MLE. In addition, the performance of the MLE becomes worse than that of the proposed algorithm when the SNR values get as small as 0 dB and the same number of frames is used because the MLE is sensitive to stationary noise.

Figure 8 illustrates how the number of data frames L_f affects the performance of our timing offset estimation when SNR = 10 dB and SNR = 20 dB, respectively. It can be seen that the proposed timing offset estimation is asymptotically unbiased and mean-squared consistent as the number of observation frames increases, which is consistent with our numerical analysis in Section 4. Under the same conditions, we can get the frequency offset estimation as shown in Figure 9. We can see that the performance of the frequency offset estimator improves when the SNR increases.

6. CONCLUSIONS

In this paper, we have proposed a low-complexity blind estimation algorithm for estimating timing offset and frequency offset in an OFDM system. An IVR, which consists of second-order statistics, can provide sufficient information to estimate the offsets. Theoretical analysis and simulation results show that the proposed estimators are asymptotically unbiased and mean-squared consistent. Furthermore, the computational complexity of the proposed schemes is lower—at least $2N_g$ times lower—than that of the MLE in [11]. In practice, the proposed estimator can serve as a coarse synchronization of the timing offset, which can quickly locate a rough search range for the fine MLE synchronization in [11]. Such a combined design can achieve the joint optimal performance in terms of both estimation accuracy and computational complexity.

REFERENCES

[1] B. Le Floch, R. Halbert-Lassalle, and D. Castelain, "Digital sound broadcasting to mobile receivers," *IEEE Trans. Consumer Electron.*, vol. 35, no. 3, pp. 493–503, 1989.

[2] C. Rapp, "Effects of HPA-nonlinearity on a 4-DPSK/OFDM-signal for a digital sound broadcasting system," in *Proc. 2nd European Conference on Satellite Communications (ECSC '91)*, pp. 179–184, Liège, Belgium, October 1991.

[3] L. J. Cimini Jr., "Analysis and simulation of a digital mobile channel using orthogonal frequency division multiplexing," *IEEE Trans. Commun.*, vol. 33, no. 7, pp. 665–675, 1985.

[4] Y. J. Kim, D. S. Han, and K. B. Kim, "A new fast symbol timing recovery algorithm for OFDM systems," *IEEE Trans. Consumer Electron.*, vol. 44, no. 3, pp. 1134–1141, 1998.

[5] M.-H. Hsieh and C.-H. Wei, "A low-complexity frame synchronization and frequency offset compensation scheme for OFDM systems over fading channels," *IEEE Trans. Veh. Technol.*, vol. 48, no. 5, pp. 1596–1609, 1999.

[6] P. H. Moose, "A technique for orthogonal frequency division multiplexing frequency offset correction," *IEEE Trans. Commun.*, vol. 42, no. 10, pp. 2908–2914, 1994.

[7] B. Park, H. Cheon, C. Kang, and D. Hong, "A novel timing estimation method for OFDM systems," *IEEE Commun. Lett.*, vol. 7, no. 5, pp. 239–241, 2003.

[8] J. J. van de Beek, M. Sandell, and P. O. Borjesson, "ML estimation of time and frequency offset in OFDM systems," *IEEE Trans. Signal Processing*, vol. 45, no. 7, pp. 1800–1805, 1997.

[9] N. Lashkarian and S. Kiaei, "Class of cyclic-based estimators for frequency-offset estimation of OFDM systems," *IEEE Trans. Commun.*, vol. 48, no. 12, pp. 2139–2149, 2000.

[10] M. J. Fernandez-Getino Garcia, O. Edfors, and J. M. Paez-Borrallo, "Frequency offset correction for coherent OFDM in wireless systems," *IEEE Transactions on Consumer Electronics*, vol. 47, no. 1, pp. 187–193, 2001.

[11] T. Lv and J. Chen, "ML estimation of timing and frequency offset using multiple OFDM symbols in OFDM systems," in *Proc. IEEE Global Telecommunications Conference (GLOBECOM '03)*, vol. 4, pp. 2280–2284, San Francisco, Calif, USA, December 2003.

[12] J.-C. Lin, "Maximum-likelihood frame timing instant and frequency offset estimation for OFDM communication over a fast Rayleigh-fading channel," *IEEE Trans. Veh. Technol.*, vol. 52, no. 4, pp. 1049–1062, 2003.

[13] T. Lv and J. Chen, "Estimation of symbol-timing and carrier-frequency offset of OFDM system over fast time-varying multipath channels," submitted to *IEEE Trans. Signal Processing*.

[14] Y-S. Choi, P. J. Voltz, and F. A. Cassara, "ML estimation of carrier frequency offset for multicarrier signals in Rayleigh fading channels," *IEEE Trans. Veh. Technol.*, vol. 50, no. 2, pp. 644–655, 2001.

[15] O. Besson and P. Stoica, "On frequency offset estimation for flat-fading channels," *IEEE Commun. Lett.*, vol. 5, no. 10, pp. 402–404, 2001.

[16] M. Luise and R. Reggiannini, "Carrier frequency acquisition and tracking for OFDM systems," *IEEE Trans. Commun.*, vol. 44, no. 11, pp. 1590–1598, 1996.

[17] Y. Li and L. J. Cimini Jr., "Bounds on the interchannel interference of OFDM in time-varying impairments," *IEEE Trans. Commun.*, vol. 49, no. 3, pp. 401–404, 2001.

Tiejun Lv received the B.S. degree from Southwest Jiaotong University, Sichuan Province, China, in 1991, and the M.S. and Ph.D. degrees in electronic engineering from the University of Electronic Science and Technology of China (UESTC) in 1997 and 2000, respectively. From January 2001 to December 2002, he was a Postdoctor in the Department of Automation, Tsinghua University, Beijing, China. Since April 2003, he has been an Associate Professor in the School of Information Engineering, Beijing University of Posts and Telecommunications (BUPT), Beijing, China. His research interests focus mainly on statistical array and signal processing for digital wireless communication systems.

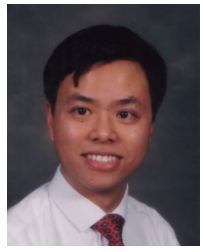

Jie Chen received his Ph.D. degree in electrical and computer engineering from the University of Maryland, College Park. He is currently an Assistant Professor at the Division of Engineering, Brown University. Dr. Chen's research interests include nanoscale devices and architecture design, genomic signal processing, and multimedia communications. He is a Distinguished Lecturer of IEEE Circuits and Systems Society (2004–2005). He has been invited as a Speaker in different conferences and workshops, and as the Guest Editor of two special issues, "Multimedia over IP" for IEEE Transactions on Multimedia and "Multimedia over Wireless Networks" for EURASIP Journal on Applied Signal Processing. Dr. Chen has published 46 scientific papers in refereed journals and conference proceedings, and the book entitled *Design of Digital Video Coding Systems: A Complete Compressed Domain Approach* (Marcel Dekker, New York, 2001); and coedited another book entitled *Genomic Signal Processing and Statistics* (EURASIP Book Series on Signal Processing and Communications, 2004). He has invented or coinvented several US Patents. He is an Associate Editor for IEEE Signal Processing Magazine, and has been an Associate Editor for IEEE Transactions on Multimedia and EURASIP Journal on Applied Signal Processing. He is a Senior Member of IEEE Signal Processing Society.

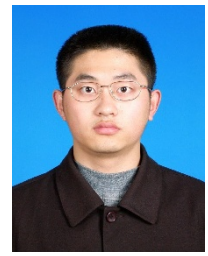

Hua Li received the B.S. degree from Wuhan University, China, in 2000, and the M.S. degree from Peking University, China, in 2003, all in electrical engineering. Since September 2004, he has been a graduate student at Brown University, USA. His research interests focus mainly on information theory and circuit design.